European Journal of Wood and Wood Products (2024) 82:2013–2028
https://doi.org/10.1007/s00107-024-02138-3

ORIGINAL ARTICLE

# Understanding the adhesion performance of glued laminated timber manufactured with Australian softwood and high-density hardwood species

A. Faircloth[1] · B. P. Gilbert[1,2] · C. Kumar[1] · W. Leggate[1,2] · R. L. McGavin[1,2]

Received: 29 May 2024 / Accepted: 14 August 2024 / Published online: 13 September 2024


**Abstract**
To be commercialised, glued laminated timber must typically conform to a strict bond integrity assessment. While the associated testing protocols vary slightly from standard to standard, the general method consists of a series of swelling (water immersion) and shrinkage (drying) cycles. The approach is independent of the species and adhesive type. Those cycles strain the gluelines to a level depending on the species' moisture uptake, timber dimensional movement and modulus of elasticity, as well as adhesive layer elasticity. High density and high modulus of elasticity materials frequently fail within the glueline regions rather than within the timber and therefore fail the bond integrity assessment. To better understand the mechanisms that lead to glueline failure, glulam samples were manufactured using three prominent Australian commercial timbers of various densities (Radiata pine—*Pinus radiata*, Southern pine—*Pinus caribaea/Pinus elliottii*, and Spotted gum—*Corymbia citriodora*) and two structural adhesive types (resorcinol formaldehyde and polyurethane). Using advanced measurement techniques (digital image correlation and strain gauges), the response of the different species and adhesive types to moisture swelling and shrinkage, as well as times at which glueline separation occurs, were captured. A relationship was observed between moisture uptake and delamination percentages with spotted gum producing significantly higher levels of delamination and significantly lower moisture uptake values, compared to both Radiata pine and Southern pine. While the polyurethane glued samples on average produced higher levels of delamination, the digital image correlation data indicates that the time at which this delamination occurs is later than the samples glued with resorcinol formaldehyde.

## 1 Introduction

Adhesive-based engineered wood products (ABEWPs) are commonly used in residential and commercial construction due to their numerous benefits, such as ease of construction, carbon sequestration and low grade feedstock utilisation (Kremer and Symmons 2018; McGavin et al. 2020). In terms of structural engineering, they provide an alternative to large cross-sections rarely found in sawn material and have reduced mechanical property variability (Nairn 2019; Sandak et al. 2020). These benefits have led to over 65% of the globally used wood products being ABEWPs (Pizzi 2016). ABEWPs face continuous technical challenges due to the ever-changing timber resource, need for processing optimisation, and new opportunities (Hunt et al. 2018). For instance, manufacturing ABEWPs from high density hardwood species in lieu of softwood creates challenges due to poor adhesive penetration and high dimensional movement, contributing to lower quality bonds when subjected to accelerated aging (Leggate et al. 2022a).

However, there is a current industry incentive to manufacture glued laminated timber (glulam) with high density Australian hardwood species. The glulam product referred to through this study consists of timber boards, face bonded to one another with each layer parallel to the last to reach a desired beam depth (WoodSolutions 2018b, 2018a). While advances in research and development have been made through focusing on the challenging aspects of adhesion, such as surface preparation, performance of different adhesive types, and the anatomical properties of different wood species (Leggate et al. 2021, 2022a), high density species are still challenging to glue. For such products to reach the

✉ A. Faircloth
Adam.Faircloth@daf.qld.gov.au

1 Queensland Department of Agriculture and Fisheries, Salisbury Research Facility, Brisbane, Australia

2 School of Engineering and Built Environment, Griffith University, Gold Coast, Australia

market, research is needed to understand the phenomenon leading to lower bond integrity and eventually find solutions for the products to pass the bond durability tests in international standards (AS/NZS 1328.1 1998; ISO 12580 2007; CSA-O112.9-04 2010; ANSI-A190.1 2017). For glulam to be considered a certified structural product in Australia, it must pass the bond durability assessment relative to its intended application in accordance with the Australia and New-Zealand standard, AS/NZS 1328.1 (1998).

The aim of this study was to analyse the strain developing during the wetting and drying stages of AS/NZS 1328.1 (1998) for different species and adhesive types to gain an understanding of the phenomena leading to delamination and when that delamination occurs. Three species of interest, Radiata Pine (RP—*Pinus radiata*), Southern Pine (SP—*Pinus caribaea/Pinus elliotti*), and Spotted Gum (SPG—*Corymbia citriodora*), were selected for this study due to their prominence on the Australian timber market and current (or desired) use as glulam. Similarly, two structural adhesives were selected for their availability and common use in glulam manufacturing which are resorcinol–formaldehyde (RF) and single component (1C) polyurethane (PUR). The paper first presents a literature review on wood adhesion (Sect. 2). The methodology is then explained in Sect. 3, consisting of (1) the material used (Sect. 3.1) and products manufactured (Sect. 3.2), and (2) the experimental tests performed including the determination of moisture content (Sect. 3.3.1), the delamination performance evaluation on the glulam specimens according to AS/NZS 1328.1 (1998) (Sect. 3.3.2), the delamination measurement through strain analysis, either using Digital Image Correlation (DIC) or strain gauges (Sect. 3.3.3) and the shear capacity changes of the gluelines after moisture cycling through block shear testing (Sect. 3.3.4). Finally, the results are presented in Sect. 4.

## 2 Literature review

The development and use of ABEWPs has been built upon for decades, however a deep understanding of wood adhesion is still lacking, and the reasons bonds can fail are often misunderstood. Investigation into the mechanisms of wood adhesion has attracted the attention of wood scientists globally (Marra 1992; Kamke and Lee 2005; Hunt et al. 2018; Nairn 2019; Leggate et al. 2020; Leggate et al. 2021; Faircloth et al. 2022; Leggate et al. 2022a). Most of these works have investigated product performance before and after being exposed to accelerated aging with limited understanding of the material performance during the exposure conditions (Hunt et al. 2018). Most standardised test methods (AS/NZS 1328.1 1998; ISO 12580 2007; CSA-O112.9–04, 2010; ANSI-A190.1, 2017) have been developed on the understanding that as timber becomes wet it weakens and swells, leading to the glueline failing as a result of the stress applied to it (River et al. 1991). This swelling process is followed by a period of drying, aimed at removing the impregnated moisture now within the sample, generating further strain distribution in the glueline through shrinkage. As the timber swells and shrinks with changes in the moisture gradient, the adhesive layer will need to either allow for movement, and/or resist the stress as a result for these actions (River et al. 1991; Frazier and Ni 1998).

Poor adhesion and minimal penetration in some high density species has been highlighted as the contributing factor for poor bonds, resulting in a mechanism referred to as "delamination" (Nairn 2019). For glulam beams in service, these delamination events are linked closely with changes in temperature and relative humidity leading to the dimensional change (shrinkage or swelling) of individual timber layers (laminates) at different rates. Nairn (2019) investigated the link between fracture mechanics and moisture change in cross laminated timber (CLT) panels. The study focused on modelling the product and material properties of the CLT and incorporated a fracture mechanics model to explain and predict delamination. Nairn (2019) found that cracks originating in the timber material and propagating toward the gluelines between layers can cause strain glueline concentrations leading to delamination. The developed model was able to predict delamination as a result of board aspect ratio, identifying that thicker boards were more likely to lead to delamination. Nairn (2019) noted that a comprehensive understanding of delamination initiation, cause, and propagation for different timber species are the prerequisites to designing durable ABEWPs. The model predicted that for a single percentage change in moisture content (MC), cracks in the wood species tested can begin to form, and for a 2–3% change in MC, delamination can start. While this study produced a detailed model, its accuracy through experimental testing has not been verified.

Although the bond durability challenge is usually more pronounced for high density timber species, the gap in understanding and visualising how the material responds to swelling and shrinkage is present for all timber species and adhesives types (Hunt et al. 2018). A review conducted by Hunt et al. (2018) considered a series of techniques and methods for further evaluation of bonded products or specifically bonded products that fail bond durability assessment in governing European standards (EN 391 and EN 14080). The review concluded there was benefit in visualising specific properties of the glueline and the surrounding timber anatomical descriptors through various techniques. Methods such as microscopy, scanning electron microscopy (SEM), and DIC were proposed to gain this deeper understanding. These techniques were found to be suitable for tracking and recording small increments of movement in the samples during their change in MC. On that note, Jonsson and Svensson

(2004) presented a method to determine the internal strain movement across the grain of glulam samples using DIC to visualise the mechanical relief along the glueline after sawing. Samples were exposed to a moisture gradient of 10% to 15% and notches were added to the ends of each glueline to force delamination to initiate at these locations. Images taken before and after sawing (placing the sawn sections back together) were able to predict internal strain of the now separated glulam by measuring the difference in pixel counts combined (Jonsson and Svensson 2004).

Building upon the findings from River et al. (1991) and Jonsson and Svensson (2004), there is a need to observe the effects various adhesives have on moisture-related strain development as well as when and where the delamination potentially begins. Knorz et al. (2016) conducted a study comparing the shear strain distribution in four prominent structural adhesives (melamine urea formaldehyde (MUF), emulsion polymer isocyanates (EPI), RF and PUR) using DIC. The impact of adhesive classification (polymerised and pre-polymerised (Hunt et al. 2018)) and glueline thickness were found to have an impact on the strain development within glulam as it dries after swelling. The results suggested strain development along the gluelines was higher for the MUF and RF adhesives when compared with the PUR and EPI (Knorz et al. 2016). The PUR and EPI type adhesives presented a poorer glueline stability as the samples took on more water (increased water uptake).

DIC is a well proven and established method for evaluating drying strain development in glulam with several studies investigating the development of strain in or around the gluelines after being subjected to a period of wetting (Gindl et al. 2005; Lanvermannet al. 2014; Sebera et al. 2015). Lee et al. (2019) compared experimental strain measurements through low temperature DIC drying analysis with shrinkage modelling predictions provided by the American Wood Council (AWC 2010). The study found similar results to Knorz et al. (2016) where the strain development and shrinkage profile were heavily dependent on species, adhesive type, and sample size. Comparing larch (*Larix kaempferi*) and pine (*Pinus koraiensis*) glulam samples, the DIC was able to accurately observe the delamination in gluelines and capture the time at which delamination occurred (Lee et al. 2019). Additionally, through the comparison of DIC analysis and the AWC (2010) predicted model, Lee et al. (2019) found that the model could be used to accurately predict dimensional change in glulam for the analysed species. While this information is useful for understanding adhesion failure types, the experiments were conducted on samples immersed through soaking only and then conditioned at moderate temperature and humidity ranges of 30 °C and 88% relative humidity (RH) [19% equilibrium moisture content (EMC)], 30 °C and 67% RH (12% EMC), 30 °C and 44% RH (8% EMC), and then oven dried. The conditioning phase for each of the above stages took 7, 4, and 2 weeks to reach 19%, 12%, and 8% EMC, respectively. These conditions are not representative of the wetting/drying conditions noted in AS/NZS 1328.1 (1998) for product quality testing and other international standards (ISO 12580 2007; CSA-O112.9–04 2010; ANSI-A190.1 2017). This limits the interpretation of the results as moisture movement will occur differently in these samples, resulting in different stresses applied to the gluelines.

## 3 Materials and methods

### 3.1 Materials

One hundred (100) linear meters of each species, i.e., RP, SP and SPG, were provided by Australian timber suppliers. Upon arrival, material was sorted to ensure no visual and surface level defects were present such as knots, splits, wane, and resin pockets as these can influence the gluability (Leggate et al. 2022a). Boards were then visually sorted to target backsawn board orientations for all species and a low proportion (less than 5%) of sapwood in the SPG boards only. Boards were prepared at 500 mm (length) × 90 mm (width) × 33 mm—RP and SP, or 22 mm—SPG (thickness) mm and conditioned in a constant environment chamber set to 20 °C and 65% relative humidity (RH). The density of the boards for each of the 3 species was determined after conditioning had taken place. This was measured in accordance with AS/NZS 1080.3 (2000). The mean and coefficient of variation (CoV) of the 3 species was *RP:* 442 kg/m$^3$ (7.34%), *SP:* 663 kg/m$^3$ (4.02%), and *SPG:* 1077 kg/m$^3$ (2.87%).

Both adhesive types were supplied by Jowat Adhesives (single component PUR—681.60 and RF (4:1 ratio of resin to hardener)—resin 950.82 and hardener 950.85).

### 3.2 Glulam manufacture

A total of thirty glulam beams (5 repeats × 3 species × 2 adhesives) were manufactured to the nominal dimensions 500 mm (length) × 90 mm (width) × 4 laminates (depth) with a total beam thickness of 132 mm for RP and SP, and the a total beam thickness of 88 mm for SPG. Note that the different thickness in the laminate used reflects the material available and commonly used by industry for each species. Immediately prior to adhesive application, the wide surfaces of the boards were face milled to remove 1.5 mm of material from each face using a Rotoles (400 D-S, Ledinek Germany) milling machine with a cutter speed of 21,000 rpm and a feed speed of 45 m/min. The boards in each sample were arranged with the growth rings showing alternative concave and convex orientations. The manufacturing process for samples using both adhesives is detailed below:

- For samples manufactured with the single component PUR, single sided application of the adhesive at a spread rate of 200 g per square meter (gsm), or 5.4 g per glueline, was used. This was followed by a press pressure of 1.0 MPa for a 2.5-h period. The time between adhesive being applied on one face and brought into contact with the mating board (referred to as open assembly time—OAT) was between 60 and 90 s. The time between glulam beam assembly (adhesive applied and boards layered) and applying pressure (closed assembly time – CAT) was 5–7 min on average.
- For samples manufactured with RF, the adhesive was first mixed at a 4:1 ratio of resin (950.82) to hardener (950.85) and left for 5–8 min to allow the adhesive to gel as suggested by the supplier. The RF mixture was applied to both mating faces in a glueline using a spread rate of 450 gsm, or 12.2 g per glueline, and pressed at 1.4 MPa overnight (minimum of 8 h). The average OAT was between 3 and 5 min and the average CAT was 10–12 min.

Beams were left to further cure for a minimum of 7 days at 20 °C and 65% RH after manufacturing before applying the cutting plan presented in Fig. 1 and testing. From this cutting plan, 4 of 75 mm (length) × 90 mm (width) × 4 laminates (thickness), and 2 of 50 mm (length) × 42 mm (width) × 4 laminates (thickness) samples were cut from the beams for testing to the methods presented in the following sections.

### 3.3 Assessment methods

This section presents a series of techniques determined from the literature and standardised testing methods to investigate various aspects of the glueline integrity of the manufactured glulam samples. The techniques provide information prior to, during, and post accelerated aging. Each of the proposed methods have been devised to assess product quality, quantify delamination location, time and rate of delamination, and monitor change in performance with different exposure conditions. The methods proposed have been executed in the order presented in Fig. 2 to allow the results of each testing procedure to inform the proceeding.

The flow of activities in Fig. 2 took place after product manufacture (detailed in Sect. 3.2):

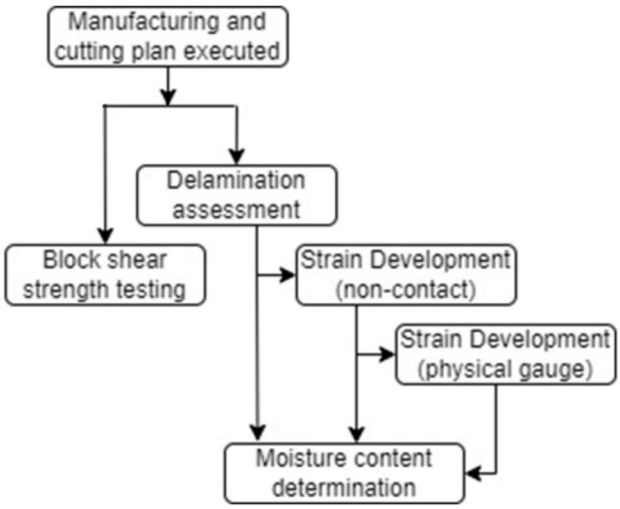


**Fig. 2** Flow chart of method completion stages and linkages

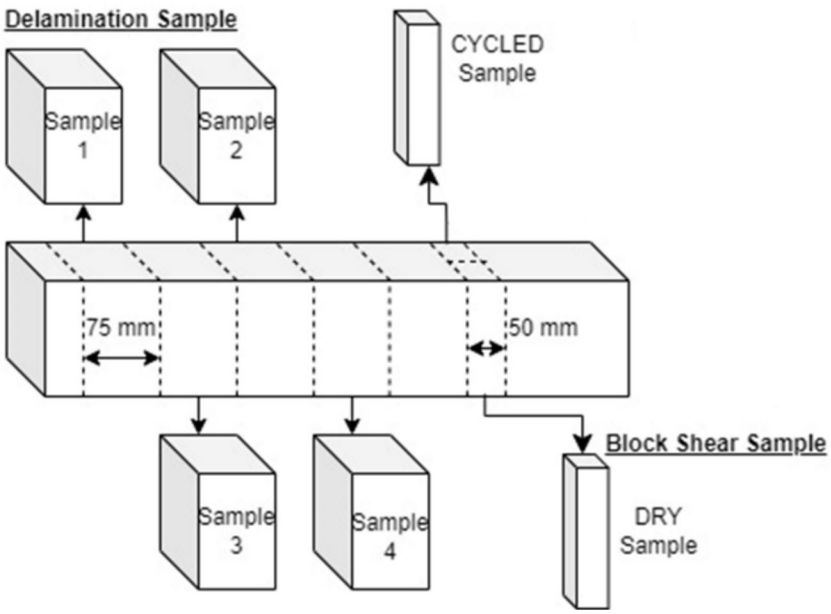


**Fig. 1** Cutting plan for sample selection showing delamination samples for AS1328.1 testing (Sample 1), DIC drying (Sample 2 and 3), strain gauge testing (Sample 4); and block shear testing (dry and cycled)

- Delamination assessment was conducted (Sect. 3.3.2) to provide the standardised performance between the different species and adhesives.
- Non-contact strain developments were measured in Sect. 3.3.3.1 during the drying phase through a DIC system which recorded the strain fields and changes in glueline integrity with changes in moisture content.
- Results of Sect. 3.3.3.1 were used to inform placement of physical strain gauges (Sect. 3.3.3.2) to complete the strain development information during the water immersion phase.
- At the conclusion of each wetting or drying phase, moisture content measurements for all samples were conducted to inform water uptake and drying quality (Sect. 3.3.1).
- Block shear specimens were tested to provide information on changes in the shear strength of the glueline before and after accelerated aging (Sect. 3.3.4).

#### 3.3.1 Moisture content determination

To determine the moisture content (MC) at the end of each of the drying and wetting phases in Sects. 3.3.2 and 3.3.3, and to back calculate the MC change through these phases, tested samples were placed in a drying oven set to 103 °C. The MC of each sample was calculated according to AS/NZS 1080.1 (2012), as,

$$MC = \frac{M_i - M_o}{M_o} \times 100\% \quad (1)$$

where $M_i$ is the mass at the time of the experiment (initial mass prior to water immersion), and $M_o$ is the mass at period of interest (actual or estimated oven dried mass).

#### 3.3.2 Delamination assessment

Thirty (30) samples referred to as "Sample 1" in Fig. 1 were assessed for delamination according to Method A of Appendix C in AS/NZS 1328.1 (1998), i.e., corresponding to an outdoor exposed product [Service Class 3 in AS/NZS 1328.1 (1998)]. It should be noted that the delamination assessment is the primary criteria for product conformance in AS/NZS 1328.1 (1998).

The following preparation and testing procedures were executed (AS/NZS 1328.1 1998):

(a) The length of each glueline on the end-grain faces for each of the conditioned samples was measured and recorded across the end-grain faces.
(b) Samples were water immersed in a vacuum/pressure cylinder by performing twice a 5-min vacuum (– 75 kPa) followed by a 1-h pressure treatment cycle (550 kPa).
(c) Samples were then dried in a kiln at 65 °C and 15% RH with an air velocity of 2.5 m/s for 21.5 h.
(d) The water immersion and drying processes in (b) and (c) were repeated to conclude 2 full treatment cycles.

At the end of each drying period in (c), the gluelines on both end-grain faces were assessed for areas of delamination. Each section of delamination in the glueline was visually marked, measured, and recorded to the nearest mm to calculate the total and maximum delamination percentages as detailed in Eq. 2 and Eq. 3, respectively (AS/NZS 1328.1 1998).

$$TotalDelamination(\%) = 100 \times \frac{l_{tot,delam}}{l_{tot,glueline}} \quad (2)$$

$$MaximumDelamination(\%) = 100 \times \frac{l_{max,delam}}{2l_{glueline}} \quad (3)$$

where $l_{total,delam}$ is the length of the total delamination (i.e., of all gluelines), $l_{total,glueline}$ is the length of all assessed gluelines measured in a), $l_{max,delam}$ is the maximum length of delamination of all measured gluelines, and $2l_{glueline}$ is two times the length of a single glueline.

Glulam assessed to Method A of Appendix C, AS/NZS 1328.1 (1998) prescribes the allowable total and maximum delamination of a glulam product as 5% (if greater than 5% but below 10% a third cycle can be performed) and 40%, respectively. Products that exceed either of these criteria are not conformant to the standard requirements.

#### 3.3.3 Strain development

Non-contact strain mapping (60 samples in total from Samples 2 and 3 in Fig. 1) and physical strain gauges (30 samples in total from Sample 4 in Fig. 1) were used to monitor the strain development during the water immersion and drying processes of Sect. 3.3.2, respectively, for each species and adhesive type.

**3.3.3.1 Non-contact strain mapping** A Correlated Solutions DIC system (Correlated Solutions, USA) was used to measure Samples 2 and 3 from Fig. 1 for dimensional changes and surface-based strain evolutions of one end-grain cross-section during the drying phase. Samples were first immersed through the process described in Sect. 3.3.2b and a random speckle pattern was then applied to the wet surface using black and white spray paint. The paint was sprayed as light as possible to keep it permeable and to ensure it did not act as a moisture barrier during drying.

The samples were then placed in a constant environment cabinet (TRH-460, Thermoline Scientific, AUS) with a glass door and individually supported on a load cell (10 kg capacity, Pavone Sistemi, Italy). The load cells were used to plot the evolution of the average moisture content in the samples based on the final moisture content calculated from Sect. 3.3.1. Four samples were tested at one time after which, new samples were submitted to the testing, until all 60 samples were tested. The chamber setpoints were set to 65 °C and 15% RH to match the settings of the drying condition set in the AS/NZS 1328.1 (1998) and used in Sect. 3.3.2 with airflow set to 2.5 m/s. However, the chamber could not reach the set temperature and relative humidity set in the standard and the actual conditions were recorded using a data logger (Hobo temperature/ relative humidity logger, Onset, USA) as 55 °C and 15% RH for the duration of the experiments, i.e., 10 °C, on average, cooler than the set point. The experimental setup is presented in Fig. 3.

The image collection was conducted using VIC-snap (version 9, Correlated Solutions, USA) with frame rates set to acquire an image every 5 min. Schneider 17 mm lenses (Xenoplan 1.4/17–0903) were attached to each of the USB 5 MP cameras (CSI-acA2440-75 µm, Basler, USA) for testing. An image resolution was 2,448 × 2,448 pixels, resulting in a pixel dimension of 71.7 µm/pixel. Other settings such as subset and step size were set to 29 and 7, respectively.

Once the experiments were completed, analysis of the images was conducted through VIC-2D (ver. 6.0.6, build 603) to evaluate the strain distributions over time. The images were first calibrated using the ruler as a scale (Fig. 3), and then a Lagrange post processing strain computation was conducted (filter size of 15).

The obtained data was used to visualise the point at which accelerated aging of the gluelines forces them to open (delaminate), the rate of delamination, and how this varies between species and adhesive type.

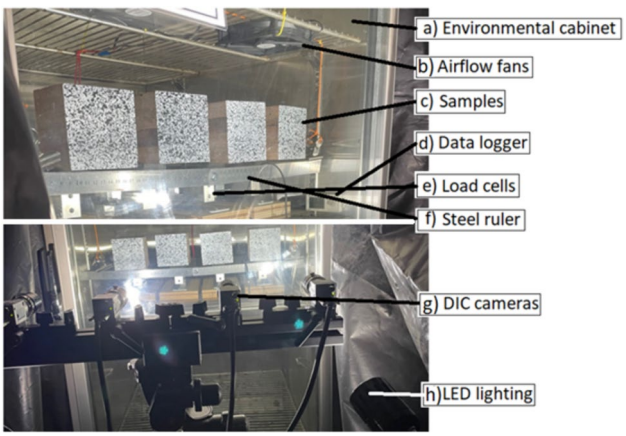


**Fig. 3** Experimental setup for cabinet drying

Analysis of the measured surface strain information was conducted as follows:

(a) The DIC results are first used to show the strain evolution of the glulam samples during the drying process. Visual observation of strain fields (ε), $\varepsilon_{xx}$ (sample width), $\varepsilon_{yy}$ (sample height), and $\varepsilon_{xy}$ (shear plane) was used to determine the plane that highlights higher levels of strain development. The $\varepsilon_{xy}$ plane was found to be the most reactive to the changes in moisture content and the drying conditions and is therefore further reported in this paper.

(b) Three virtual extensometers were then placed along the middle glueline, typically experiencing the highest levels of strain as informed by the previous analysis. The extensometers were 5 mm in length and evenly spaced 10 mm apart from each other at the positions shown in Fig. 4.

(c) The time at which delamination occurs along with the delamination rate (i.e., evolution) are reported in this paper based on the virtual extensometers. The increase in displacement of the extensometers reflects delamination initiation and propagation.

**3.3.3.2 Physical strain gauge measurement** Physical strain gauges were used on 30 samples through this section to monitor the strain build up during the swelling/shrinkage phase of testing outlined in point (b) of Sect. 3.3.2. The strain gauges are well suited for this phase as they are waterproof, can compensate for temperature and do not need visual access to the samples, as the DIC does. Strain gauge placement was informed by the DIC results where locations along the glueline that were seen to experience higher level of strains during drying were targeted. The selected positions were 20 mm from the sample edge on the second glueline and in the centre of the second board (see Fig. 5) to allow for the effective placement of the gauge (based on its surface area coverage) and to capture where drying stress is considered related to the glueline interface and less influenced by the edge faces. Furthermore, the particular positioning was reinforced from the results of Sect. 3.3.3.1 which were conducted prior to sample preparation for this section. Bi-axial

**Fig. 4** Virtual extensometer inspection points

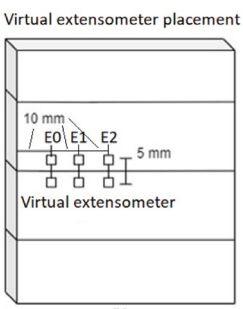

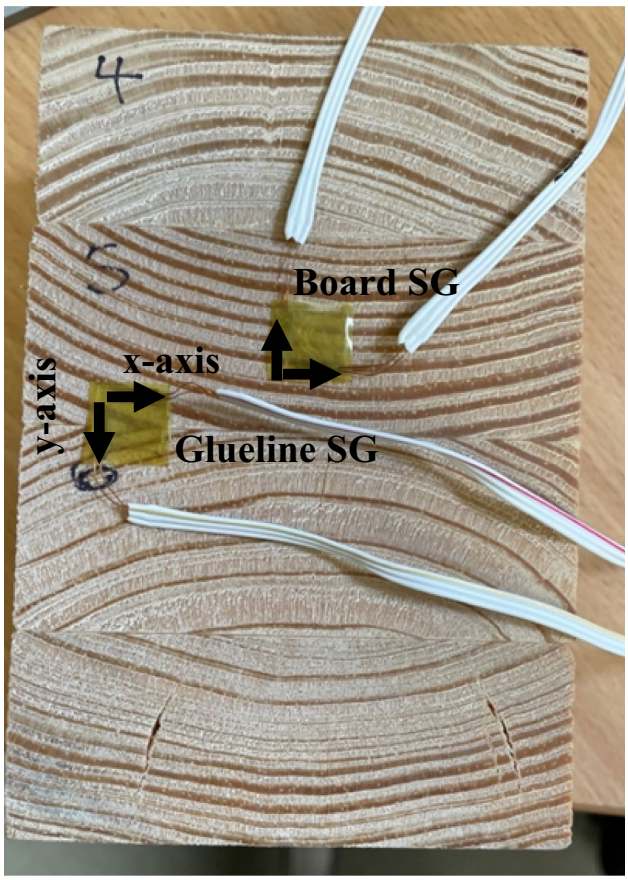


**Fig. 5** Strain gauge positioning on samples

SGs (5 mm gauge length, 120Ω, 2.06-gauge factor, Kyowa, Japan) were used to capture the strain in the two directions parallel to the sample edges. The strain gauged surfaces were prepared by first sanding them with 40 grit sandpaper followed by bonding the SGs to the prepared area using an epoxy resin adhesive (CC-36X5, Kyowa Electronic Instruments, Japan). A secondary (dummy) gauge unattached to the glulam sample surface was placed alongside the test sample and was used to compensate the strain calculations for any temperature influence. Information was captured at 5-min intervals.

#### 3.3.4 Block shear strength

To determine the effect of the swelling and shrinkage cyclic treatments on the shear capacity of the glueline and to gain further understanding on the glueline quality for all species and adhesives investigated, block shear strength testing was conducted according to Appendix D of AS/NZS 1328.1 (1998). Visual wood fibre assessment (WFA) of the separated glueline according to ASTM D5266-13 (2020) was also performed to estimate the wood failure percentage. As presented in Fig. 1, two samples from the 50 mm section were extracted for testing, corresponding to 30 samples for each of the two tested conditions. One of the samples was tested prior to cyclic treatment (referred to as 'DRY') and the second directly after being exposed to the cycling treatment explained in b) through d) of Sect. 3.3.2, i.e. two full cycles (referred to as 'CYCLED').

The block shear tests were carried out using a block shear jig (as presented in Fig. 6) in a Universal Testing Machine (Shimadzu AG–X, Japan) fitted with a 100 kN load cell and tested at a stroke rate of 1.5 mm/min.

Each glueline of the block shear sample was tested consecutively with the maximum load at failure ($F_{max}$) for each glueline recorded. $F_{max}$ was then used to calculate the shear

**Fig. 6** **a** Block shear schematic, and **b** testing setup

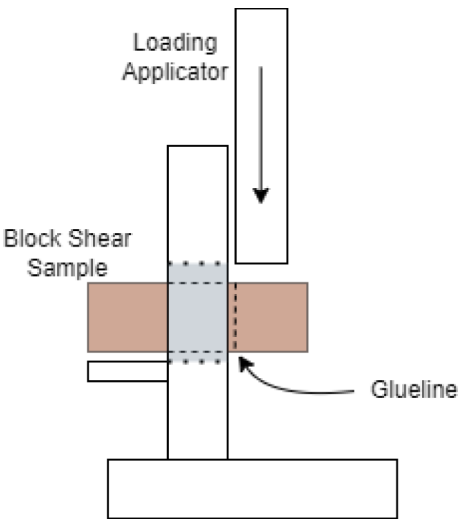


(a)

(b)

strength ($f_v$) of each glueline according to Eq. 4 (AS/NZS 1328.1 1998), as,

$$fv = \frac{Fmax}{A} \quad (4)$$

where $A$ is the measured cross-sectional area of the glueline.

Each sheared glueline was then assessed in accordance with ASTM D5266-13 (2020) to visually estimate the percentage of remaining wood failure percentage adhered at the glueline proportional to the entire glueline surface to the nearest 5% due to the subjective visual assessment method in the standard (0% referred to no wood failure and 100% referring to total wood failure). Figure 7 presents examples of the wood failure percentage of 0, 25, 50, 75, and 100% coverage.

### 3.4 Statistics

A pairwise t-test was performed with a 95% confidence level to test for the presence of a significant difference between groups for glueline delamination (total and maximum), block shear strength, and WFA. Statistical interpretation was conducted through the use of RStudio (ver. 1.3.1058).

## 4 Results and discussion

### 4.1 Delamination assessment

Table 1 presents the summarised results for the maximum and total delamination assessments in accordance with Appendix C of AS/NZS 1328.1 (1998) for each full treatment cycle. The results are provided based on species and adhesive. The results have been reported as the mean and coefficient of variation (CoV) percentage values for the dataset with statistical analysis performed on the total delamination only.

According to the assessment criteria outlined in AS/NZS 1328.1 (1998), the maximum delamination (i.e., in a single glueline) values are below the 40% allowable delamination threshold for all adhesives and species tested. The pass/fail criteria are then controlled by the total delamination values. For the two adhesive types, RP would pass (below 5%) the total delamination criteria noted in AS/NZS 1328.1 (1998) as would the RF SP samples. On the other hand, the SPG would fail (greater than 5%) the


**Fig. 7** Examples of wood failure percentage for visual interpretation of wood fibre assessment **a** 0%, **b** 25%, **c** 50%, **d** 75%, and **e** 100%

**Table 1** Summary of the total and maximum delamination results for the various species, adhesives, and cycles—mean values for the total delamination followed by the same subscript letter are not significantly different (p-value > 0.05)

| | Total delamination | | | Maximum delamination | | |
|---|---|---|---|---|---|---|
| | RP | SP | SPG | RP | SP | SPG |
| PUR - 1st Cycle | | | | | | |
| Mean (%) | $0.0^{g}$ | $5.4^{d}$ | $54.8^{b}$ | 0.0 | 4.3 | 35.1 |
| CoV (%) | 0 | 7.5 | 22.4 | 0 | 5.3 | 23.2 |
| PUR - 2nd cycle | | | | | | |
| Mean (%) | $1.1^{g}$ | $9.2^{c}$ | $61.7^{a}$ | 1.0 | 6.8 | 38.5 |
| CoV (%) | 2.2 | 8.5 | 18.6 | 2 | 5.9 | 9.7 |
| RF - 1st Cycle | | | | | | |
| Mean (%) | $0.0^{g}$ | $0.6^{g}$ | $66.4^{a}$ | 0.0 | 0.6 | 38.0 |
| CoV (%) | 0 | 1.4 | 20.5 | 0 | 1.4 | 30.8 |
| RF - 2nd cycle | | | | | | |
| Mean (%) | $2.9^{ef}$ | $3.6^{e}$ | $69.3^{a}$ | 2.2 | 2.6 | 39.4 |
| CoV (%) | 4.2 | 4.4 | 18.1 | 3.1 | 3.2 | 8.7 |

total delamination criteria. The following points arise from analyses applied to the total delamination results:

- For the 1st cycle, PUR SP samples present significantly higher levels of delamination ($t(8) = 4.24$, $p = 0.001$), compared to their RF SP counterparts. However, PUR SPG samples presented significantly lower levels of delamination ($t(8) = -1.02$, $p = 0.019$) compared to RF SPG samples. The RP samples did not delaminate for both adhesives after 1 cycle.
- For the 2nd cycle, no significant difference was noted between adhesives for the SPG samples ($t(8) = -0.81$, $p = 0.221$). PUR RP presented significantly lower ($t(8) = -1.20$, $p = 0.013$) levels of delamination compared to the corresponding RF samples while the PUR SP ($t(8) = 2.04$, $p = 0.019$) samples presented significantly higher levels of delamination compared to the RF samples.
- Comparing the difference in delamination between cycles, no significant difference was noted for the RF SPG ($t(8) = -0.25$, $p = 0.404$) and PUR RP ($t(8) = -2.44$, $p = 0.056$) samples. However, the remaining samples all presented significantly higher levels of delamination after a second cycle, when compared with the first (PUR SP ($t(8) = 2.46$, $p = 0.049$), PUR SPG ($t(8) = 0.76$, $p = 0.023$), RF RP ($t(8) = 2.02$, $p = 0.039$), and RF SP ($t(8) = 2.08$, $p = 0.036$)).

These delamination results and interpretations appear consistent with Leggate et al. (2022a) who found difficulties in forming effective bonds with high density materials as a result of poor adhesive penetration. Findings for the lack of significant change between cycles for the SPG samples may suggest that the stresses exerted on the glueline reached a maximum after an initial cycle and are not exceeded after during the second cycle, or that too much delamination had already developed in the first cycle to release the stresses away from the gluelines.

## 4.2 Moisture content determination

Figure 8 shows the evolution of the average change in MC for the whole sample over the duration of the first drying cycle (Item c) in Sect. 3.3.2) for each species. As the movement of moisture through these samples is species specific (not affected by adhesive), RF and PUR samples were combined for the analysis. Also, as the second moisture cycle showed similar results to the first cycle, it is not presented herein for clarity. Figure 8 presents a final dried average total MC of 16.4%, 14.1%, and 9.81% for RP, SP, and SPG, respectively.

Differences between drying curves for the three species confirm that SP and RP are significantly more permeable than SPG. Moisture uptake (i.e., the moisture absorbed by the samples during the wetting cycles reflected by the initial MC content of the drying cycle) results showing no significant difference between RP and SP ($t(38) = 2.08$, $p = 0.222$). However, SPG showed an overall MC variation of 7.2% between beginning of the drying cycle to the end, significantly lower when compared to 91.6% and 71.9% for the RP and SP samples, respectively. This suggests that the SPG samples are not taking up or losing moisture at the same rate than the other two species, therefore creating different stress patterns between species. For all species, it was estimated that the samples lose 50% of their MC in the first 8 h of the 21 h drying cycle.

## 4.3 Strain development

### 4.3.1 Non-contact strain mapping

Figure 9 presents the DIC mapped strain ($\varepsilon_{xy}$) frames taken at 30 min, 8 and 21 h during drying for RP, SP and SPG. These

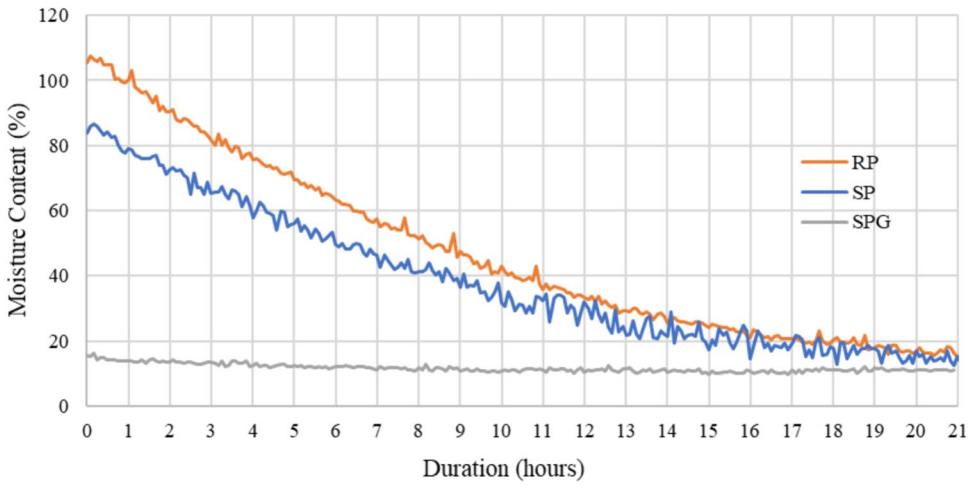


**Fig. 8** Drying curves for the average MC change over time of RP, SP, and SPG samples

images are considered representative and were selected to provide a visual description of the differences the two species groups (hardwoods and softwoods) experience in regard to strain development during accelerated aging. These times have been selected as representative of the initial, mid and final drying stages in terms of MC change according to the data plotted in Fig. 8. No major differences in strain development were observed between the two adhesives for the three species and thus only PUR images are presented in Fig. 9. It is noted that as cracks developed in the samples, the DIC showed high strain data around the cracks which do not represent the actual strain value in the material. Indeed, the software calculates the strain over a speckled area which include the crack opening, leading to unrealistic strain value at these locations, but it represents a useful tool to visualise the crack locations. From the images shown in Fig. 9, delamination can be seen for the RP and SPG samples with some level of delamination noted in SP. Cracks developing in the timber itself along the tangential grain direction can also be seen. The level of strain in the RP samples, representative of the level of crack opening, at the end of the drying process appears greatest at the 1st and 2nd gluelines, i.e., the gluelines closest to the drying fan (see also extensometer readings hereafter). The SPG samples presented delamination at the 8 h point (Fig. 9h) with minimal visual difference between the 8 (Fig. 9h) and 21 (Fig. 9i) hour images.

In some instances, the delamination caused continuously too much separation along the glueline which the DIC could no longer track (resulting in the areas no longer covered by the strain mapping field of view). When delamination developed, in all cases it was found to initiate at the edges of the glueline and propagate towards the centre of the samples (specifically notable in Fig. 9b, c). This was found consistent for all samples showing delamination however the time at which delamination began varied as detailed later with the analysis of the extensometers.

Figure 10 presents the virtual extensometer readings placed along the glueline versus time for each species and adhesive type. The samples selected to generate the plots in Fig. 10 were ones with signs of delamination. The direction of strain used to generate the plots in Fig. 10 was in the y-axis direction similar to the physical gauges shown in Fig. 5. The plots show that for both RP and SP no delamination occurred in the first 5–10 h at the strain gauges i.e. positioned at 10, 20, 30 mm from the edge, until a point is reached when the extensometer reading increases reflecting the delamination initiation and propagation verified through visual observation. Delamination develops later for the RP samples, as reflected in the strain mapping discussion in the paragraph above. The SPG however shows almost immediate delamination as seen in the strain mapping images. Table 2 provides the average time at which delamination began for all samples.

Both RF RP and RF SPG presented a significant difference in delamination occurrence with their respective PUR samples (RP: $t(18) = -2.25$, $p = 0.017$, SPG: $t(18) = -3.36$, $p = 0.002$), with delamination occurring earlier than the PUR samples. SP however, presented no significant difference ($t(18) = -0.76$, $p = 0.231$) between RF and PUR samples for delamination initiation. These findings suggest that the rigid bonds achieved from the RF adhesive result in bondline cracking earlier than the PURs due to their lower elastic modulus (Knorz et al. 2016).

#### 4.3.2 Physical strain gauge measurement

Figure 11 presents typical strain gauge data obtained through the water immersion testing for RP, SP, and SPG samples. The data collected from the bi-axial strain gauges was evaluated and the direction that experienced higher levels of strain was considered. Figure 11a shows representative examples of the strain development perpendicular to the glueline (y-axis strain gauge) for the 3 species and Fig. 11b shows similar examples of strain development parallel to the board width (x-axis strain gauge). No difference was noted between adhesive types; therefore, results have been reported irrespective of adhesive.

Due to the larger moisture intake of the RP and SP samples when compared to SPG (see Fig. 8), and with the three species not presenting widely different swelling coefficients per moisture content (SPG: tangential – 0.38%, radial – 0.32%; SP: tangential – 0.29%, radial – 0.20%; RP: tangential – 0.27%, radial – 0.20% (QTimber; WoodSolutions; Hopewell 2001; QDAFF 2013)), the strain development over time in both Fig. 11a, b shows higher strain level in the RP and SP, and minimal change in strain for SPG. A plateau point in both Fig. 11a, b through the water immersion period for SP and RP is noted where the samples appear to no longer develop strain as a result of likely reaching the fibre saturation point.

### 4.4 Block shear assessment

#### 4.4.1 Block shear strength

Figure 12 and Fig. 13 present the distribution of block shear strength values for each tested species and adhesive type across the DRY and CYCLED testing conditions, respectively. The results are further summarised in Table 3. The outliers in the DRY RF SPG (Fig. 12) samples represent the maximum and minimum of the distribution.

The following arise from the statistical analyses from the data presented in Figs. 12, 13 and Table 3:

- A general observation from the DRY results presented in Fig. 12 is that the mean shear strength appears to follow

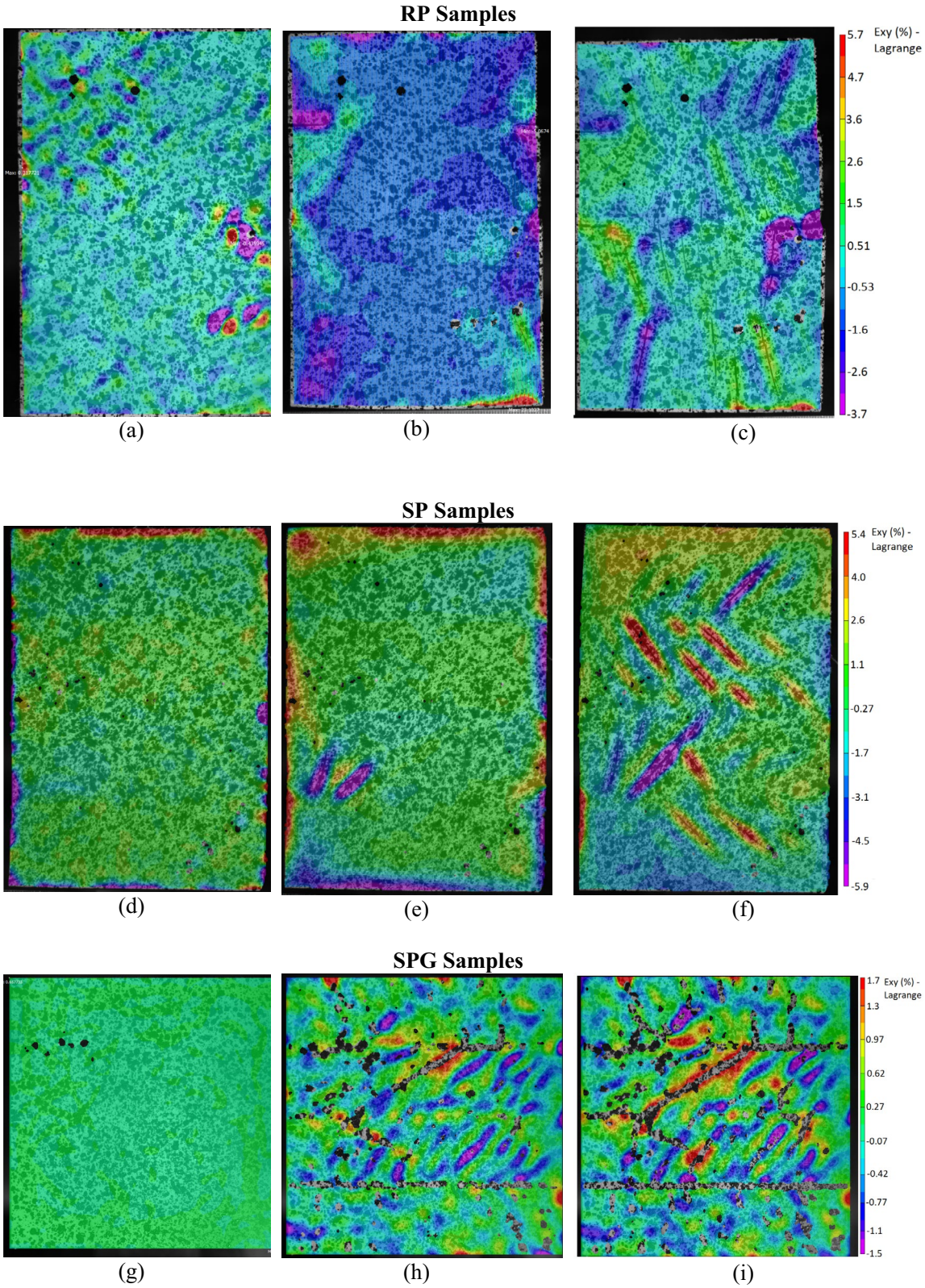


**Fig. 9** DIC output images from $\varepsilon_{xy}$ strain field during the first drying cycle for a RP sample at **a** 30 min, **b** 8, **c** and 21 h, a SP sample at **d** 30 min, **e** 8, and **f** 21 h, and a SPG sample at **g** 30 min, **h** 8, **i** and 21 h

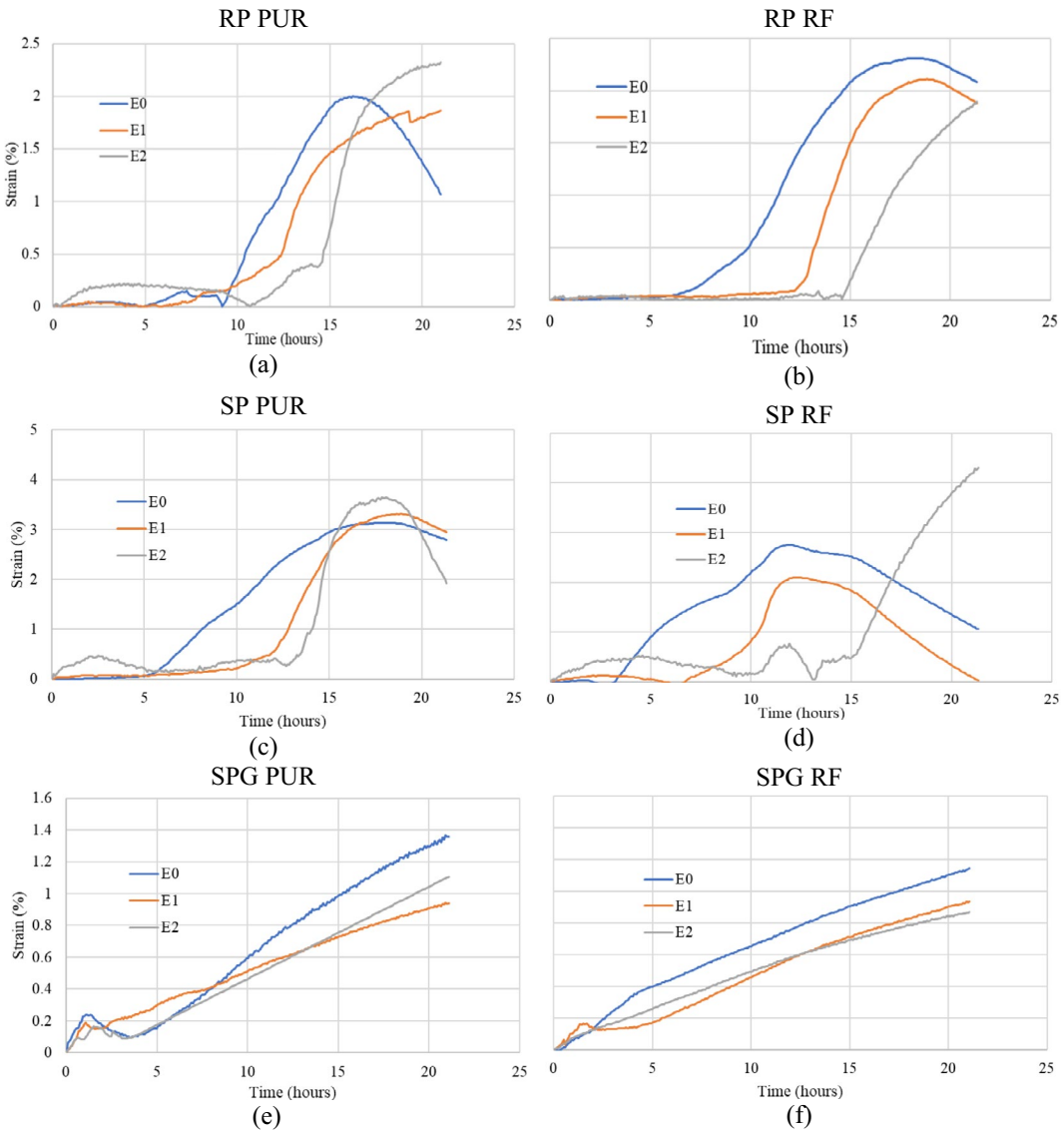


**Fig. 10** Example of selected strain gauge development over time for (a) PUR RP, (b) RF RP, (c) PUR SP, (d) RF SP, (e) PUR SPG, (f) and RF SPG

the density of the tested materials irrespective of adhesive type, i.e. SPG is the highest density material and returns the highest shear strength values, RP is the lowest density and as such returns the lowest shear strength.

- In the DRY condition, the SPG RF results present significantly higher shear strength ($t(8) = -3.80$, $p = 0.003$) when compared with PUR samples with a mean shear strength of 16.7 MPa and 13.0 MPa, respectively. The DRY RP ($t(8) = 0.48$, $p = 0.323$) and DRY SP ($t(8) = 0.36$, $p = 0.486$) samples show no significant difference between mean shear strength values when comparing PUR and RF adhesives.
- Fig. 13 shows no visible relationship between shear strength and density after the CYCLED treatment for PUR samples, however the RF samples show the inverse relationship between shear strength and density that was reported for the DRY results of Fig. 12, i.e. CYCLED SPG (highest density) RF samples produced the lowest shear strength, and RP which is lowest density reported the highest shear strength values.
- For the CYCLED condition in Fig. 13, SPG PUR samples present significantly higher shear strength values compared SPG RF samples ($t(8) = 2.77$, $p = 0.012$) with a mean shear strength of 8.32 MPa and 5.95 MPa, respectively. This is inverse to the DRY condition results.
- CYCLED samples for RP and SP present no significant difference in shear strength ($t(8) = -0.25$, $p = 0.403$ and

**Table 2** Summary results from DIC assessment for first delamination time—mean values followed by the same subscript letter are not significantly different (p-value > 0.05)

| Species | Adhesive | | Delamination time (hours) |
|---|---|---|---|
| RP | PUR | Mean (h) | 17.2[a] |
| | | CoV (%) | 12.6% |
| | RF | Mean (h) | 14.2[b] |
| | | CoV (%) | 17.8% |
| SP | PUR | Mean (h) | 9.50[c] |
| | | CoV (%) | 14.6% |
| | RF | Mean (h) | 9.58[c] |
| | | CoV (%) | 28.9% |
| SPG | PUR | Mean (h) | 3.84[d] |
| | | CoV (%) | 23.6% |
| | RF | Mean (h) | 1.88[e] |
| | | CoV (%) | 17.0% |

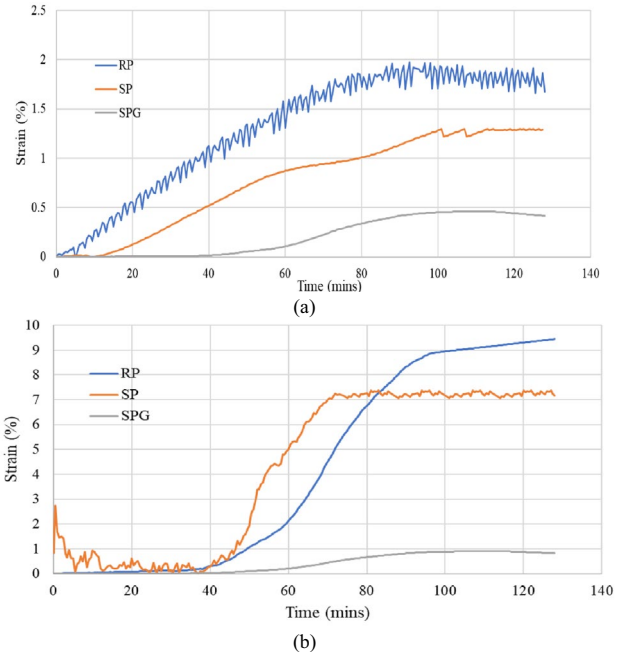


**Fig. 11** Representative strain development over time for RP, SP, and SPG for a) the gluelines, and b) the board

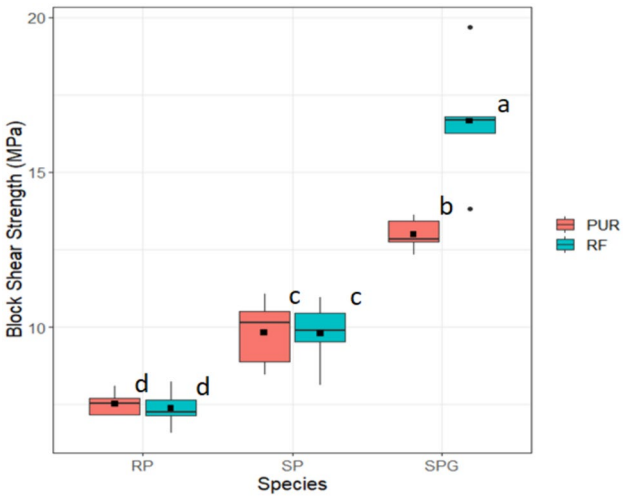


**Fig. 12** Block shear strength distribution for SPG, SP and RP with PUR and RF adhesive under DRY testing conditions (Box distribution plots followed by the same letter are not significantly different; p-value > 0.05)

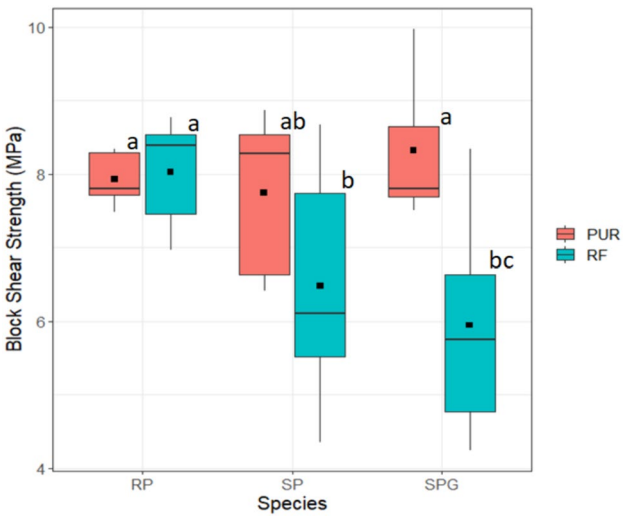


**Fig. 13** Block shear strength distribution for SPG, SP and RP with PUR and RF adhesive under CYCLED testing conditions (Box distribution plots followed by the same letter are not significantly different; p-value > 0.05)

t(8) = 1.37, p = 0.104, respectively) between PUR and RF adhesives.

- Comparing the results of DRY and CYCLED, RP shows minimal change between adhesives with a mean difference of 5.0% and 8.1% between PUR and RF, respectively.
- The performance ratio values for both SP and SPG indicate a typical reduced shear strength for the RF adhesive type when compared to the PUR in the CYCLED condition, especially for the SPG samples. The CoV is also higher for the RF samples showing greater variation for the adhesive after CYCLED condition testing. The RP however, shows a near 1.0 performance ratio (expected by the lack of significant change in results between CYCLED and DRY results). However the CYCLED samples for both adhesives do present increased CoVs.

Comparing the trends of the shear strengths with those obtained from delamination measurements, no relationship

**Table 3** Summarised block shear strength for both DRY and CYCLED results

| Species | Adhesive | DRY (MPa) | CYCLED (MPa) | Performance Ratio (CYCLED/DRY) |
|---|---|---|---|---|
| RP | PUR | 7.53$^{d}$ (0.61) | 7.93$^{d}$ (0.63) | 1.05 |
| | RF | 7.37$^{d}$ (0.78) | 8.03$^{d}$ (1.40) | 1.09 |
| SP | PUR | 9.81$^{c}$ (3.42) | 7.75$^{d}$ (18.1) | 0.79 |
| | RF | 9.86$^{c}$ (6.18) | 6.48$^{de}$ (21.7) | 0.66 |
| SPG | PUR | 13.0$^{b}$ (1.25) | 8.32$^{cd}$ (11.7) | 0.64 |
| | RF | 16.7$^{a}$ (4.76) | 5.95$^{e}$ (25.3) | 0.36 |

Values presented in parenthesis are the CoV (%). Mean values followed by the same subscript letter are not significantly different (p-value > 0.05)

can be found to link the two. This lack of relationship between shear strength and delamination suggests the glueline failures are caused through a motion other than shear. Lu et al. (2024) also concluded this where after conducting fracture energy experiments using bonded SPG specimens. Similar studies on the performance of bonded wood products found complimentary results where CYCLED testing presents a significant decrease in bond performance compared to DRY results (Klausler et al. 2013; Leggate et al. 2022b; Faircloth et al. 2023). The SPG samples present much higher shear strength values compared to both SP and RP in the DRY condition but lower or equal shear strength in the CYCLED condition.

#### 4.4.2 Wood fibre assessment (WFA)

Table 4 presents the WFA from the block shear samples tested in Sect. 4.4.1.

Through the statistical analyses, the following points are outlined:

- No significant difference for the WFA of RP RF ($t(8) = 1.94$, $p = 0.088$) and SP RF ($t(8) = -0.281$, $p = 0.393$) between DRY and CYCLED conditions were identified. The SPG samples for the RF adhesive show a significant difference ($t(8) = 7.02$, $p = 5.5e\text{-}5$) between DRY and CYCLED in WFA with a factor 4.8 decrease.
- The SP PUR samples show a significant decrease between DRY and CYCLED ($t(8) = 7.70$, $p = 2.86e\text{-}5$) with a 32% difference, however no significant difference was noted between the treatment types for RP PUR ($t(8) = -1.65$, $p = 0.068$) and SPG PUR ($t(8) = -0.67$, $p = 0.262$).

The low WFAs of the SPG samples is expected to be a result of poor adhesive penetration; a noted cause of low wood failure percentage bonded in hardwoods (Faircloth et al. 2023; Leggate et al. 2022a). There appears to be no relationship between shear strength and WFA for the DRY state with SPG producing the highest shear strength values and lowest WFA percentages. SP however shows the highest WFA and the second highest shear strength values.

## 5 Conclusion

This study discusses the bond integrity of glulam manufactured using three important, Australian commercial timbers (RP, SP, and SPG), with two structural adhesives (PUR and RF). The study investigated the performance of these products for a service class 3 exposure condition described in AS/NZS 1328.1 (1998). The findings of the study are summarised as follows.

- Delamination assessment after a single cycle found significantly higher rates of delamination for SPG compared to both SP and RP, irrespective of adhesive. RP samples presented little to no delamination irrespective of adhesive. Two cycles resulted in a slight increase in total delamination for all permutations and species however not meaningfully different to what was reported after a single cycle.
- The relationship between moisture and strain of the 3 tested species identified both RP and SP to have an average moisture uptake approximately 5 times higher than SPG, leading to higher dimensional movement overall.
- The DIC strain analysis for all samples enabled the visualisation of the crack development in the timber material as well as delamination in the gluelines. Results showed that delamination initiates at the extremities of

**Table 4** Summarised WFA data for the block shear testing

| Mean | WFA (%) | | | | | |
|---|---|---|---|---|---|---|
| | PUR | | | RF | | |
| | RP | SP | SPG | RP | SP | SPG |
| DRY | 64.0$^{c}$ (20.9) | 95.0$^{e}$ (8.47) | 15.0$^{e}$ (13.2) | 90.7$^{a}$ (7.94) | 82.7$^{ab}$ (16.2) | 49.3$^{d}$ (31.0) |
| CYCLED | 76.7$^{bc}$ (12.1) | 65.0$^{c}$ (15.5) | 15.0$^{e}$ (18.5) | 83.4$^{ab}$ (21.7) | 84.3$^{ab}$ (10.2) | 10.3$^{e}$ (6.71) |

Values presented in parenthesis are the CoV (%)—mean values followed by the same subscript letter are not significantly different (p-value > 0.05)

the glueline and propagates through to the sample centre. Delamination develops early for the SPG samples, typically 2.8 h after the start of the drying cycle, while signs of delamination for the other two species typically develops in 13.4 h.

- The PUR and RF SPG CYCLED samples presented a 36% and 64% decrease in block shear strength, respectively, when compared to the DRY samples. A similar trend was observed for the SP samples with the SP PUR shear strength decreasing by 21% and the SP RF by 34%. The RP samples present no notable change between the two tested conditions for the two tested adhesives.

**Acknowledgements** The authors would like to acknowledge the funding support received for this research, provided through the Australian Centre for International Agricultural Research (ACIAR) project titled "Coconut and other non-traditional forest resources for the manufacture of engineered wood products" (FST/2019/128). Additionally, acknowledgements are due to the Queensland Department of Agriculture and Fisheries (DAF) and their expansive capacity at the Salisbury Research Facility. The technical support and advice of key industry partners such as Jowat Adhesives (Mr Rodney Vella), and Robertson Brothers Sawmill is acknowledged. Dr Peraj Karbaschi, Mr Paul Chan and Mr Andrew Outhwaite from DAF are recognised for their contributions towards the data collection and assessment.

**Author contributions** Adam Faircloth: Conceptualisation, methodology development, manufacturing, experimental testing, analysis, writing and editing. Benoit P. Gilbert: Analysis, writing, reviewing, and editing. Chandan Kumar: Analysis, writing, reviewing, and editing. William Leggate: Supervision, conceptualisation, funding acquisition, reviewing, and editing. Robbie L. McGavin: Supervision, conceptualisation, funding acquisition, reviewing, and editing.

**Funding** Open Access funding enabled and organized by CAUL and its Member Institutions.

**Data availability** Data will be made available upon request.

## Declarations

**Conflict of interest** The authors declare no conflict of interest.



## References

ANSI-A190.1 (2017) Standard for wood products—structural glued laminated timber. APAwood, Tacoma

AS, NZS1328.1 (1998) Glued laminated structural timber, Part 1: Performance requirements and minimum production requirements. Standards Australia/ Standards New Zealand, Sydney

AS, NZS1080.3 (2000) Timber—methods of test, part 3: density. Standards Australia/ Standards New Zealand, Sydney

AS, NZS1080.1 (2012) Timber—methods of test, method 1: moisture content. In Standards Australia/ Standards New Zealand, Sydney

AWC (2010) American Wood Council. Retrieved from https://awc.org/. Accessed 24 April 2024

CSA-O112.9-04 (2010) Evaluation of Adhesives for Structural Wood Products (Exterior Exposure). Canadian Standard Association Group, Ottawa

D5266-13, A (2020) Standard practice for estimating the percentage of wood failure in adheisve bonded joints. ASTM International, West Conshohocken

Faircloth A, Outhwaite A, Leggate W (2022) adhesives reserach for softwood and hardwood engineered wood products. South and Central Queensland Forestry Hub-Timber Queensland. Retrieved from https://www.qldforestryhubs.com.au. Accessed 11 Aug 2022

Faircloth A, Kumar C, McGavin R, Leggate W, Gilbert BP (2023) Mechancial performance and bond integrity of finger jointed high-density sub-tropical hardwoods for residential decking. For MDPI. https://doi.org/10.3390/f14050956

Frazier CE, Ni J (1998) On the occurrence of network interpenetration in the wood-isocyanate adhesive interphase. Int J Adhesion Adhesives 18(2):81–87. https://doi.org/10.1016/S0143-7496(97)00048-1

Gindl W, Stretenovic A, Vincenti A, Muller U (2005) Direct measurement of strain distribution along a wood bond line. Part 2: effects of adhesive penetration on strain distribution. Holzforschung 59(3):307–310. https://doi.org/10.1515/HF.2005.051

Hopewell G (2001) Characteristics, utilisation and potential markets for Cape York Peninsula Timbers. Retrieved from Brisbane, Australia

Hunt CG, Frihart CR, Dunky M, Rohumaa A (2018) Understanding wood bonds—going beyond what meets the eye: a critical review. Rev Adhesion Adhesives 6(4):369–440. https://doi.org/10.7569/RAA.2018.097312

ISO 12580 (2007) Timber structures—glued laminated timber—methods of test for glue-line delamination. International Standards Organisation, Geneva

Jonsson J, Svensson S (2004) A contact free measurement method to determine internal stress states in glulam. Holzforschung 58:148–153. https://doi.org/10.1515/HF.2004.022

Kamke FA, Lee NJ (2005) Adhesive penetration in wood—a review. Wood Fiber Sci 39(2):205–220

Klausler O, Rehm K, Elstermann F, Niemz P (2013) Influence of wood machining on tensile shear strength and wood failure percentage of one-component polyurethane bonded wooden joints after wetting. Int Wood Prod J 5(1):18–26. https://doi.org/10.1179/2042645313Y.0000000039

Knorz M, Niemz P, Kuilen JW (2016) Measurement of moisture-related strain in bonded ash depending on adhesive type and glue-line thickness. Holzforschung 70(2):145–155. https://doi.org/10.1515/hf-2014-0324

Kremer P, Symmons M (2018) Perceived barriers to the widespread adoption of mass timber construction: an Australian Construction Industry Case Study. Mass Timber Constr J 1:1–8

Lanvermann C, Sanabria SJ, Mannes D, Niemz P (2014) Combination of neutron imaging (NI) and digital image correlation (DIC) to determine intra-ring mositure variation in Norway spruce. Holzforschung 68(1):113–122. https://doi.org/10.1515/hf-2012-0171

Lee SS, Pang SJ, Jeong GY (2019) Effects of size, species, and adjacent lamina on moisture-related strain in glulam. Wood Fiber Sci 51(2):1–18. https://doi.org/10.22382/wfs-2019-013

Leggate W, McGavin RL, Miao C, Outhwaite A, Chandra K, Dorries J, Knackstedt M (2020) The influence of mechanical surface preparation methods on southern pine and spotted gum wood properties: wettability and permeability. BioResources 15(4):8554–8576. https://doi.org/10.15376/biores.15.4.8554-8576

Leggate W, McGavin RL, Outhwaite A, Kumar C, Faircloth A, Knackstedt M (2021) Influence of mechanical surface preparation methods on the bonding of southern pine and spotted gum: tensile shear strength of lap joints. BioResources 16(1):46–61. https://doi.org/10.15376/biores.16.1.46-61

Leggate W, McGavin RL, Outhwaite A, Gilbert B, Gunalan S (2022a) Barriers to the effective adhesion of high-density hardwood timbers for glue-laminated beams in Australia. MDPI for 13(1038):1–14. https://doi.org/10.3390/f13071038

Leggate W, Outhwaite A, McGavin RL, Gilbert BP, Gunalan S (2022b) The effect of the addition of surfactants and the machining method on the adhesive bond quality of spotted gum glue-laminated beams. BioResources 17(2):3413–3434. https://doi.org/10.15376/biores.17.2.3413-3434

Lu P, Gilbert BP, Kumar C, McGavin RL, Karampour H (2024) Influence of the moisture content on the fracture energy and tensile strength of hardwood spotted gum sawn timber and adhesive bonds (gluelines). Eur J Wood Prod 82:53–68. https://doi.org/10.1007/s00107-023-01999-4

Marra AA (1992) Technology of wood bonding: principles and Practice. Van Nostrand Reinhiold

McGavin RL, Dakin T, Shanks J (2020) Mass-timber Construction in Australia: Is CLT the only answer? Bioresources.com 15(3):4642–4645. https://doi.org/10.15376/biores.15.3.4642-4645

Nairn JA (2019) Predicting layer cracks in cross-laminated timber with evaluations of strategies for supressing them. Eur J Wood Prod 77:405–419. https://doi.org/10.1007/s00107-019-01399-7

Pizzi A (2016) Wood products and green chemistry. Ann for Sci 73:185–203. https://doi.org/10.1007/s13595-014-0448-3

QDAFF (2013) Southern Pine (plantations). Retrieved from State of Queensland

QTimber. Available online: https://qtimber.daf.qld.gov.au/browse-timbers. Accessed 28 June 2023

River BH, Vick C, Gillespie RH (1991) Wood as an Adherend. In: Mindford JD (ed) Treatise on Adhesion and Adhesives. Elsevier, Berlin, pp 1–238

Sandak A, Brzezicki M, Sandak J (2020) Trends and perspectives in the use of timber and derived products in building facades. New Mater Civ Eng 11:333–374. https://doi.org/10.1016/B978-0-12-818961-0.00009-0

Sebera V, Muszynski L, Tippner J, Noyel M, Pisaneschi T, Sundberg B (2015) FE analysis of CLT panel subjected to torsion and verified by DIC. Mater Struct 48:451–459. https://doi.org/10.1617/s11527-013-0195-1

WoodSolutions (2018a) Cross Laminated Timber (CLT). www.woodsolutions.com.au/wood-species/wood-products/cross-lamianted-timber-clt. Accessed 8 Jul 2022

WoodSolutions (2018b) Glued Laminated Timber (Glulam). www.woodsolutions.com.au/glulam-glued-laminated-timber. Accessed 8 Jul 2022

WoodSolutions. Available online: https://www.woodsolutions.com.au/wood-species. Accessed 28 June 2023